

Howard Baer<sup>1</sup>, Michal Břihák<sup>1</sup>, Chih-hao Chen<sup>1;2</sup> and Xerxes Tata<sup>3</sup>

<sup>2</sup>Davis Institute of High Energy Physics, University of California, Davis, CA 95616, USA

(March 26, 2022)

We investigate the experimental implications of the minimal gauge-mediated low energy supersymmetry breaking (GMLESB) model for Fermilab Tevatron collider experiments. We map out the regions of parameter space of this model that have already been excluded by collider searches and by limits on  $b \rightarrow s$ . We use ISAJET to compute the cross sections for a variety of topological signatures which include photons in association with multiple leptons, jets and missing transverse energy. The reach in the parameter space, which fixes the scale of sparticle masses, is estimated to be 60, 100 and 135 TeV for Tevatron integrated luminosities of 0.1, 2 and 25 fb<sup>-1</sup>, respectively. The largest signals occur in photon(s) plus lepton(s) plus multi-jet channels; jet-free channels containing just photons plus leptons occur at much smaller rates, at least within this minimal framework.

1

## I. INTRODUCTION

The search for weak scale supersymmetry (SUSY) [1] forms an integral part of the experimental program [2] at all high energy colliders in operation or in the construction and planning phases. In the absence of any one compelling theoretical framework, the experimental analyses have to be performed within the context of particular models. The Minimal Supersymmetric Standard Model (MSSM) is obtained by the direct supersymmetrization of the Standard Model (SM), but with two Higgs doublets, and including all renormalizable soft supersymmetry breaking interactions consistent with SM symmetries. The resulting theory has over one hundred model parameters making phenomenological analyses intractable. (If R-parity violation by renormalizable baryon- (or lepton-) number violating superpotential interactions is allowed, the number of model parameters is even larger.) The proliferation of soft-SUSY breaking parameters is a reflection of our lack of understanding of the mechanism of SUSY breaking. The practical solution for reducing the parameter space is to incorporate simplifying ansatzes usually based on the assumed symmetries of physics at very high scales.

One especially attractive and economic realization of this idea is provided by the so-called minimal supergravity (mSUGRA) framework [3] that has been recently used for most phenomenological [2], and also some experimental [4], analyses of SUSY. Here, "minimal" refers in part to the technical assumption of canonical kinetic energy terms. It is envisioned that SUSY is dynamically broken at a scale  $M_{\text{SUSY}}$  in a sector of the theory that interacts with the observable sector of quarks, leptons, gauge and Higgs bosons and their superpartners only via gravity, which acts as the "messenger" of supersymmetry breaking [5]. As a result the particle-particle mass gap in the observable sector is suppressed by  $\frac{1}{M_P}$  relative to  $M_{\text{SUSY}}$  and is thus given by  $M_{\text{SUSY}}^2 = M_P$ . This quantity may be of order the weak scale if  $M_{\text{SUSY}}$  is  $10^{11}$  GeV, where the reduced Planck mass  $M_P = 2.4 \cdot 10^8$  GeV. The Goldstone fermion (which dominantly lives in the hidden sector) then forms the longitudinal components of the gravitino which generically acquires a mass  $M_{\text{SUSY}}^2 = M_P$  by the super-Higgs mechanism [6]. Although a weak scale particle, the couplings of the gravitino are of gravitational strength, so that it plays no role in particle physics. The resulting low energy Lagrangian [5] in the observable sector is just a globally supersymmetric Lagrangian with universal scalar ( $m_0$ ) and gaugino masses ( $m_{1=2}$ ) and a universal trilinear scalar soft-SUSY breaking parameter ( $A_0$ ) at an ultra-high scale  $M_X$  often identified with  $M_{\text{GUT}}$ . The universality of the gaugino mass may have its origins in grand unification while the universal boundary condition for the scalar masses results from our technical assumption of the canonical kinetic energy terms, mentioned above. Although these boundary conditions are not generic [7] to supergravity models (and are tantamount to assuming an additional global symmetry known to be broken by Yukawa interactions) this framework is generally referred to as the minimal SUGRA framework. A very attractive feature of this picture is that over a significant portion of the parameter space of the model, radiative corrections lead to the correct pattern of electroweak symmetry breaking [8]; the SUSY Higgs mass parameter  $^2$  is then fixed by the value of  $M_Z$ . In such a scenario, all the sparticle properties are determined by just four additional parameters along with  $\tan \beta$ . The lightest supersymmetric particle (LSP) is frequently the lightest neutralino ( $\tilde{\chi}_1^0$ ) and is a good candidate for cosmological cold dark matter if R-parity is conserved as is assumed to be the case [9].

Attractive though this framework is, it says nothing about the dynamics of SUSY break-

ing. In recent studies, Dine, Nelson, Nir and Shirman [10] have attempted to construct models where SUSY is dynamically broken in the hidden sector of the theory and communicated to a messenger sector via new gauge interactions. The messenger sector, which is characterized by a mass scale  $M$ , interacts with the observable sector via the known SM gauge interactions which then serve to communicate SUSY breaking to the visible sector quarks, leptons, gauge and Higgs bosons, and their superpartners. The effective SUSY breaking scale in the observable sector is now suppressed by  $M$  rather than  $M_P$  and is  $\frac{1}{4} M_{SUSY}^2 = M^2$ , with  $M_{SUSY}$  being the induced SUSY breaking scale in the messenger sector and  $\frac{1}{4}$  is the relevant SM one structure constant. The effective scale of SUSY breaking in the observable sector may thus be  $M_{weak}$  even if the SUSY breaking scale and the messenger scale  $M$  are as small as few tens or few hundred TeV. The gravitino mass, which is still suppressed by  $M_P$ , is smaller by a factor  $M = M_P \cdot 10^{-12}$  compared to  $m_G$  within the SUGRA framework for  $M = 250$  TeV. Thus in these new scenarios, the gravitino mass may be in the electron-volt range. Fayet [11] has shown that for the longitudinal components of such a superlight gravitino the smallness of the gravitational coupling is made up by the size of the wavefunction of the gravitino of electroweak scale energy so that this gravitino does not decouple from other particles.

The fact that the gravitino, and not the lightest neutralino, is the LSP is the main reason why the phenomenology of these models can be quite different [12{14] from the usual MSSM analyses. Most importantly, the lightest neutralino (as well as other neutralinos) can now decay via  $\tilde{\chi}_1^0 \rightarrow \gamma$ , and also via  $\tilde{\chi}_1^0 \rightarrow \gamma Z$  or  $\tilde{\chi}_1^0 \rightarrow \gamma H_i$  (where  $i = \ell, h$  or  $p$  for light, heavy and pseudoscalar Higgs bosons) if the decays are kinematically allowed. We will see that for sparticle masses accessible at the Tevatron, the photon decay dominates over much of the parameter space of the model. Since the gravitino escapes experimental detection, we expect that in such a scenario SUSY events will generically have the  $n$ -jet(s) +  $m$ -lepton(s) +  $k$ - $\gamma$  +  $E_T$  topology. We find that the branching ratio for sparticles other than  $\tilde{\chi}_1^0$  to decay via the gravitino mode is small, so that  $k = 0$ –2 because the photon detection efficiency is not unity. This novel source of photons in SUSY events was considered [12{14] to be the origin of the single  $e^+e^- + E_T$  event [15] recorded by the CDF Collaboration. Finally, we will show that at least within the simplest of the gauge mediated low energy SUSY breaking (GMLESB) models reviewed in the next Section, there would have been a plethora of other events accompanying the CDF event, making its SUSY origin within this context rather implausible.

The scenarios envisioned in Ref. [10] are in a sense considerably more ambitious than the conventional SUGRA picture since they include not only a mechanism for the transmission of SUSY breaking, but also the dynamical mechanism for it. Thus, all scales in the low energy theory, in particular the values of  $\mu$  and the SUSY breaking Higgs boson mass parameters that describes the observable sector, should be derived in such a scenario. Since there is no universally accepted resolution of the  $\mu$  problem [16], we will adopt a phenomenological approach and focus on the implications of the GMLESB model, treating  $\mu$  to be a parameter that gets fixed by the value of  $M_Z$  via the constraint from radiative electroweak symmetry breaking [14]. In other words, we regard the mediation of SUSY breaking and the mechanism of SUSY breaking as independent issues, with independent consequences.

The remainder of this paper is organized as follows. In Section II we briefly review the assumptions underlying the GMLESB model and set up the parameter space for our

phenomenological analysis. We delineate the regions of parameter space already excluded by experiments at LEP 2 and the measurement of the  $b \rightarrow s$  branching ratio by the CLEO Collaboration. Finally, in Sec. II we study the branching fractions for the direct decays of sparticles to gravitinos which is the novel feature of these scenarios. In Section III, we use ISAJET [17] to generate events which lead to the various  $n \rightarrow j + m \rightarrow k + \bar{k} + \bar{p}$  event topologies at the Fermilab Tevatron and give an estimate of its reach in various channels from the data of Run I as well as from Run II with the Main Injector and the proposed [18] TeV 33 upgrade. We summarize our results in Section IV.

## II. THE MINIMAL MODEL OF GAUGE MEDIATED SUPERSYMMETRY BREAKING

### A. Model Parameter Space

Supersymmetry is dynamically broken in the "secluded sector" (this was referred to as the hidden sector in the SUGRA framework) of the theory and communicated to the "messenger sector" via some new gauge interactions which do not couple to the known particles. In the simplest realization of this idea [10] the messenger sector is weakly coupled [19] (so that non-perturbative dynamics does not cause SUSY breaking via gaugino masses) and comprises of one set of "quark" and "lepton" superfields in a  $5 + \bar{5}$  representation of  $SU(5)$  coupled to a singlet via a superpotential of the form  $W = g_1 \hat{S} \hat{q} \hat{q} + g_2 \hat{S} \hat{l} \hat{l}$ . The incorporation of new fields in complete GUT multiplets ensures that they do not spoil the successful prediction of  $\sin^2 \theta_w$  if this model is incorporated into a GUT. The scalar and auxiliary components of the field  $\hat{S}$  acquire vacuum expectation values,  $\langle h \rangle$  and  $\langle F \rangle$ , the latter signalling the breaking of SUSY in the messenger sector. SM gauge interactions then carry the information of SUSY breaking to the observable sector, and induce masses (proportional to the corresponding  $\beta$  function structure constant) for the gauginos via one loop quantum corrections. The chiral scalars feel the effect of SUSY breaking only via these gaugino masses, so that SUSY breaking scalar squared masses are induced only as two loop effects. If  $\langle F \rangle = \langle h \rangle^2$ , the gaugino and scalar masses are respectively given by [10],

$$m_{\tilde{g}} = \frac{1}{4} g^2 ; \quad (2.1)$$

and

$$m_{\text{scalar}}^2 = 2 g^2 C_3 \left(\frac{3}{4}\right)^2 + C_2 \left(\frac{2}{4}\right)^2 + \frac{3}{5} \left(\frac{Y}{2}\right)^2 \left(\frac{1}{4}\right)^2 ; \quad (2.2)$$

with  $g = \langle F \rangle / \langle h \rangle$ , and  $C_1$  given in terms of the usual hypercharge coupling  $g^0$  by  $C_1 = \frac{5}{3} \frac{g^0}{4}$ . Finally,  $C_3 = \frac{4}{3}$  for colour triplets and zero for colour singlets while  $C_2 = \frac{3}{4}$  for weak doublets and zero for weak singlets. These relations, which are independent of the messenger sector superpotential couplings  $g_{1,2}$ , get corrections of  $\mathcal{O}\left(\frac{\langle F \rangle}{\langle h \rangle^2}\right)$  which are ignored in the subsequent analysis. Notice that instead of a universal scalar mass as in SUGRA, the masses of the scalars in this model depend on their gauge quantum numbers: squarks are the heaviest, followed by uncoloured electroweak doublets, followed by the colour and electroweak singlets. Since the gaugino masses are radiatively generated [20], the mass

relation is exactly as in a GUT model, although the physics behind this is very different. SUSY breaking  $A$ -parameters and the  $B$ -parameter are induced only at higher loops so that it is reasonable to suppose that these are small. The supersymmetric parameter is not determined by how SUSY breaking is mediated but will be fixed (up to a sign) by the constraints of radiative symmetry breaking as in the SUGRA framework. A complete theory that includes the dynamics of SUSY breaking will presumably yield a value of consistent with this.

Eq. (2.1) and Eq. (2.2) should be regarded as boundary conditions for the gaugino and scalar masses valid at the messenger scale  $M = \hbar \text{Si}$  (we assume  $e_1 = e_2$ ), so that these parameters need to be evolved down to the weak scale relevant for phenomenological analysis. The renormalization group evolution (RGE) of various SUSY breaking gaugino and scalar masses is illustrated in Fig. 1, assuming the boundary conditions discussed above. In this example we have chosen  $\sqrt{s} = 40 \text{ TeV}$ ,  $M = 500 \text{ GeV}$ ,  $\tan \beta = 2$  and taken  $\mu < 0$ . The top mass is fixed to  $m_t = 175 \text{ GeV}$  throughout this paper. As expected the squarks, on account of their QCD interactions, are significantly heavier than all the other scalars. The SUSY breaking  $t$ -squark masses are smaller than those for other squarks on account of their large Yukawa interactions which reduce their masses as  $Q$  is evolved down to the weak scale. The right-handed sleptons which have only hypercharge gauge interactions are considerably lighter than the left-handed slepton or Higgs doublets. Finally, the running gaugino masses are proportional to the corresponding fine structure constants at all scales. The most important feature of Fig. 1 is that  $m_{H_u}^2$  becomes negative and electroweak symmetry is radiatively broken just as in SUGRA models. Then, we can eliminate the weak scale  $B$ -parameter in favour of  $\tan \beta$  (we will return to the issue of whether the resulting value of  $B$  evolved to the scale  $M$  is compatible with the expectation from the boundary condition) while  $\mu^2$  is determined by  $M_Z^2$ . In doing so, we have minimized the one-loop corrected effective potential. The model is thus completely specified by the parameter set  $(\sqrt{s}, \tan \beta, M, \text{sgn } \mu)$ . The dependence on  $M$  is presumably logarithmic since it only enters via the boundary conditions, so that the  $\mu$  vs:  $\tan \beta$  plane provides a convenient arena for presenting our results.

## B. Sparticle Masses and Experimental Constraints

We begin by showing contours of various sparticle masses and the weak scale SUSY parameters  $A_t$  and  $\mu$  in the  $\mu$  vs:  $\tan \beta$  plane for the two signs of  $\mu$ . We show contours of  $m_{\tilde{g}}, m_{\tilde{u}_L}, m_{\tilde{u}_R}$  and  $m_{\tilde{\chi}_R}$  in Fig. 2a for  $\mu < 0$  and Fig. 2b for  $\mu > 0$ . In Fig. 2c and Fig. 2d we show contours for  $m_{\tilde{q}}$  and  $m_{\tilde{g}}$  in addition to contours for  $A_t$  and  $\mu$  for the two signs of  $\mu$ . We have fixed  $M = 500 \text{ TeV}$ .

The region in Fig. 2 denoted by bricks is where the proper breaking of electroweak symmetry is not obtained. The hatched region is where the lightest neutral Higgs boson  $m_{H_0} < 60 \text{ GeV}$  or  $m_{\tilde{u}_L} < 79 \text{ GeV}$ . The latter bound has recently been obtained by the ALEPH collaboration at LEP2 [21]. The chargino bound is derived assuming that the chargino is gaugino-like with  $m_{\tilde{u}_L} = m_{\tilde{e}_L} = 10 \text{ GeV}$ , and further that the  $\tilde{\chi}_1^\pm$  escapes detection. Although no analyses have been specially carried out for the GMLESB scenario, the clean experimental environment makes it difficult to imagine that these chargino signals would have evaded detection even if  $\tilde{\chi}_1^\pm$  were unstable and decayed within the detector via

$\tilde{Z}_1 \rightarrow \gamma$ . The LEP limit of  $m_H > 63$  GeV has been obtained for a SM Higgs boson; our corresponding requirement of  $m_{H^\pm} > 60$  GeV for the light MSSM Higgs boson should be an excellent approximation for the GMLESB framework since the additional Higgs bosons are all comparatively heavy (see below). The cross-hatched region at large  $\tan\beta$  is where  $m_{\tilde{\chi}_1} < m_{\tilde{Z}_1}$  (recall that  $\tilde{\chi}_1 \rightarrow \tau$  mixing can be substantial for large values of  $\tan\beta$ ). While this last region would have been excluded by cosmological considerations within the mSUGRA framework, this is not so for the GMLESB model since the  $\tilde{\chi}_1$  is unstable. Indeed, if the model parameters are in the cross-hatched region the phenomenology will be quite different. Charginos and neutralinos (including  $\tilde{Z}_1$ ) will cascade decay to  $\tilde{\chi}_1$  which will then decay via  $\tilde{\chi}_1 \rightarrow \gamma$  with a width (independent of stau mixing) given by

$$(\tilde{\chi}_1 \rightarrow \gamma) = \frac{1}{48} \frac{(m_{\tilde{\chi}_1}^2 - m^2)^4}{m_{\tilde{\chi}_1}^3 M_P^2 m_G^2} \quad (2.3)$$

which yields a decay length of  $\sim 1.8 \times 10^3 \tau_{\tilde{\chi}_1} (m_{\tilde{\chi}_1}=100 \text{ GeV})^5 (m_G=1 \text{ eV})^2 \text{ cm}$ . Thus, for this region of parameters, every SUSY event will contain 2-4  $\gamma$ 's in the final state instead of hard isolated photons. We will not elaborate this scenario any further.

The following features of Fig. 2 are worth noting.

The scale of particle masses is set by  $\mu$ . Except for the cross hatched region,  $\tilde{Z}_1$  is the next-to-lightest particle (NLSP), and further, except for  $\tan\beta$  close to unity, particle masses are insensitive to  $\tan\beta$ .

The left-handed sleptons (and sneutrinos) are substantially heavier than  $\tilde{\chi}_R$ ; squarks are generally heavier than gluinos except for third generation squarks which have substantial Yukawa interactions (see Fig. 1). It is worth mentioning that the ratio  $\frac{m_q}{m_g}$ , (at the scale  $M$ ) decreases as the square root of the number of SU(5) vector multiplets in the messenger sector [12], and can go below unity. If the number of messenger sector fields is large, this will effect the phenomenology which is sensitive to whether squarks are decaying into gluinos or vice-versa. A similar comment applies to slepton and electroweak gaugino masses.

The value of  $\mu$  which is obtained from radiative symmetry breaking is large so that the lighter chargino and the two lightest neutralinos are gaugino-like, while  $\tilde{W}_2$  and  $\tilde{Z}_{3,4}$  contain large Higgsino components. Thus the chargino and neutralino mass and mixing patterns are qualitatively similar to those in the mSUGRA model.

Even though we start with  $A_t(M) = 0$ , an  $A$ -parameter of several hundred GeV is generated by the renormalization group running: since  $\mu$ ,  $A_t$  and  $m_{\tilde{t}_{L,R}}$  have comparable magnitudes, there is considerable mixing in the  $t$ -squark sector.

Although we have not shown this, all but the lightest of the neutral Higgs scalars tend to be heavy. We have checked that these are always heavier than 180 GeV, and frequently much heavier. Again, this feature is common with the mSUGRA model. Of course, the Higgs sector may be sensitive to any re-norments designed to solve the  $\mu$  problem.

The CLEO Collaboration [22] has quoted the 95% CL range  $1 \cdot 10^{-4} < \mathcal{B}(b \rightarrow s \gamma) < 4 \cdot 10^{-4}$  from their study of inclusive flavour changing neutral current decays of  $B$ -mesons. Such low energy measurements provide constraints on any particular model framework where virtual effects of new particles can contribute to the decay. We have used the recent analysis described in Ref. [23] to compute this branching fraction within the GMLESB framework. The result of this computation is illustrated in the  $\mu$  vs:  $\tan \beta$  plane in Fig. 3 for (a)  $\mu < 0$ , and (b)  $\mu > 0$ . Again, we have fixed  $M = 500$  TeV. This constraint excludes a substantial region of the parameter space for negative  $\mu$  due to constructive interference amongst the various SUSY and SM loop contributions. The CLEO experiment poses no constraint for  $\mu > 0$ , since in this case the various SUSY loops contributions interfere destructively. The rate for  $b \rightarrow s \gamma$  could be sensitive to the modifications of the Higgs sector arising from new dynamics included to generate  $\mu$  dynamically. For this reason, in Sec. III we include in our study parameter space points for which this  $b \rightarrow s \gamma$  constraint is not satisfied.

Before turning to phenomenology, we note that the conditions for electroweak symmetry breaking determine [14] the weak scale  $B$  in terms of  $\tan \beta$  (while  $\mu$  is fixed by the value of  $M_Z$ ). This value of  $B$  can then be evolved to  $B_0$ , its value at the messenger scale  $M$ . Since  $B_0$  is not generated at one loop, we expect that it should be small within our framework. Contours of  $B_0$  are shown in the  $\mu$  vs:  $\tan \beta$  plane in Fig. 4 for (a)  $\mu < 0$ , and (b)  $\mu > 0$ . We see that for positive values of  $\mu$ ,  $B_0$  is always very large. On the other hand, there is a region of parameter space with  $\mu < 0$  where  $B_0$  is close to zero. If we take the model literally, we would conclude that  $\tan \beta$  is fixed to be between 20 and 30, depending on the value of  $\mu$  and  $\mu < 0$ . While this might be interesting in itself, this conclusion would probably be altered by the addition of new interactions that would be necessary to generate  $\mu$  dynamically. For this reason we will remain agnostic about  $\tan \beta$  and  $\mu$  in the remainder of this paper.

### C. The decay of the Lightest Neutralino

We have seen that below the scale  $M$ , the GMLESB model looks just like the minimal supersymmetric model with (correlated) soft supersymmetry breaking terms, together with a very light gravitino as the LSP. The NLSP, which is usually the  $\tilde{\chi}_1$ , thus decays via  $\tilde{\chi}_1 \rightarrow \tilde{G}$  and also via  $\tilde{\chi}_1 \rightarrow Z \tilde{G}$  and  $\tilde{\chi}_1 \rightarrow H_i \tilde{G}$  if these decays are kinematically allowed. Expressions for these decay rates are given in Ambrosanio et. al. [13] and will not be repeated here.

The branching fractions for the various decays are shown versus  $\mu$  in Fig. 5 for (a)  $\tan \beta = 2$ ;  $\mu < 0$ , (b)  $\tan \beta = 2$ ;  $\mu > 0$ , (c)  $\tan \beta = 10$ ;  $\mu < 0$  and (d)  $\tan \beta = 10$ ;  $\mu > 0$ . The messenger scale has been fixed at our canonical choice  $M = 500$  TeV. We see that the photonic branching fraction dominates for the entire range of  $\mu$  even though  $m_{\tilde{\chi}_1}$  is as heavy as 180 GeV for  $\mu = 140$  TeV. This is a reflection of the fact that  $\tilde{\chi}_1 \rightarrow \tilde{B}$ . Since the zino component of  $\tilde{B}$  is suppressed relative to the photino component by  $\tan \beta$ , we expect that  $\mathcal{B}(\tilde{\chi}_1 \rightarrow \tilde{G} Z)$  is suppressed by a factor  $\sin^2 \beta$ . The remaining suppression comes from the strong  $\alpha_s$  suppression of these decays. The decay rate to  $H_i$  is negligible because the Higgsino component of  $\tilde{\chi}_1$  is tiny.

The decay length  $L = \frac{1}{\Gamma_{\tilde{\chi}_1 \rightarrow \tilde{G}}} c$  of the neutralino is illustrated in Fig. 6 for (a)  $M = 500$  TeV with  $\mu < 0$ , (b)  $M = 5000$  TeV with  $\mu < 0$ , (c)  $M = 500$  TeV with  $\mu > 0$  and (d)  $M = 5000$  TeV with  $\mu > 0$ . The curves are for three different values of  $\frac{E}{m_{\tilde{\chi}_1}} = 1.5; 2$

and 4, (from bottom to top). In this plot, we have fixed  $\tan\beta = 2$ . We expect our results are insensitive to this choice as long as  $\tilde{E}_1 \ll \tilde{B}$ . We see that for our canonical choice  $M = 500$  TeV, the decay length varies from a fraction of a millimeter to a few centimeters. Thus the neutralinos will decay inside the detector and the displaced vertices from which a high energy photon shower emerges could provide additional confirmation of this scenario. For the larger value of  $M$  shown, the decay length could be as large as several meters if  $\tilde{B}M$  is small, so that the neutralino would decay outside the detector. In this case, the topological signatures would be similar to those in the minimal model: the vestiges of the GMLESB model would show up only via the particle mass patterns. Intermediate values of  $M$  could cause the  $\tilde{E}_1$  to mainly decay outside the electromagnetic calorimeter, or within the muon chamber. Whether these decays can be readily identified and/or the photon energy measured is an important experimental issue. It is interesting to note that while the particle mass scale provides a handle on  $\tilde{B}$ , a measurement [24] of the decay length of  $\tilde{E}_1$  would directly yield information about the messenger scale, particularly if the composition of the  $\tilde{E}_1$  could be determined from other experiments.

### III. SIGNALS FROM THE GMLESB MODEL AT THE TEVATRON

The patterns of particle masses, and hence, the cross sections for various particle processes can be quite different from expectations in, for instance, the mSUGRA framework. In order to compute these cross sections as well as to generate SUSY events at the Tevatron within the GMLESB model framework, we have interfaced the output for the various weak scale parameters as obtained by RGE, starting from the GMLESB boundary conditions with ISAJET [17]. We begin by showing in Fig. 7 the cross sections for various SUSY processes as a function of  $\sqrt{s}$  for the same cases (a)–(d) shown in Fig. 5. Again, we have fixed  $M = 500$  TeV. We use the CTEQ2L structure functions [25] for our computations. We show the cross sections for the dominant  $\tilde{W}_1\tilde{E}_2$  and  $\tilde{W}_1\tilde{W}_1$  processes separately, and group together the processes of slepton and sneutrino pair production in the figure. The curve labelled "Other" refers to other chargino and neutralino processes while "Assoc." refers to the production of a gluino or squark in association with a chargino or a neutralino. We note the following.

Over the complete range of  $\sqrt{s}$  where the cross sections are potentially observable,  $\tilde{W}_1\tilde{E}_2$ ,  $\tilde{W}_1\tilde{W}_1$  and slepton/sneutrino production processes dominate. The production of gluinos and squarks is always subdominant. This is a reflection of the fact that gluinos and squarks are rather heavy even for the smallest allowed value of  $\tilde{B}$ .

The strongly interacting particles get rapidly heavier as  $\tilde{B}$  increases, so that their cross sections drop off faster for a fixed collider energy. For the same reason, the production cross section for electroweak particles falls off the slowest, with the associated production cross sections in between.

The cross section for the production of "other" charginos and neutralinos is significant for smaller values of  $\sqrt{s}$  shown, particularly if  $\tilde{B} > 0$ . Presumably, this is because  $\tilde{B}$  is not overwhelmingly large and gaugino-Higgsino mixing tends to reduce the particle masses.



## A . Event Simulation

For each set  $(\mu, \tan\beta, M, \text{sgn})$ , of input G M L E S B parameters, our R G E program yields a set of weak scale S U S Y parameters. We use these as an input to I S A J E T to generate S U S Y events at the Tevatron. Thus, for any set of G M L E S B parameters I S A J E T generates all  $2 \times 2$  S U S Y processes (those mediated by s-channel Higgs production must be run separately) with appropriate cross sections, and decays all sparticles as in the minimal S U S Y model. The decay  $\tilde{\chi}_1^0 \rightarrow \gamma$  with a branching fraction of 100% (this is an excellent approximation as can be seen from Fig. 5) is added to the I S A J E T decay table. Gravitino decays of sparticles other than  $\tilde{\chi}_1^0$  are ignored [26].

To model the experimental conditions at the Tevatron, we use the toy calorimeter simulation package I S A P L T. We simulate calorimetry covering  $4\pi$  with a cell size given by  $\Delta\eta = 0.1$   $\Delta\phi = 0.0875$ , and take the hadronic (electromagnetic) calorimeter resolution to be  $\frac{\Delta E}{E} = \frac{0.15}{\sqrt{E}}$  ( $\frac{0.15}{\sqrt{E}}$ ). Jets are defined as hadronic clusters with  $E_T > 15$  GeV within a cone of  $R = \sqrt{\Delta\eta^2 + \Delta\phi^2} = 0.7$  with  $j_{T,j} > 3.5$ . Muons and electrons with  $E_T > 7$  GeV and  $j_{T,j} < 2.5$  are considered to be isolated if the visible hadronic  $E_T$  within a cone of  $R = 0.3$  about the lepton direction is smaller than 5 GeV. We identify photons within  $j_{T,j} < 1$  if  $E_T > 12$  GeV, and consider them to be isolated if the additional  $E_T$  within a cone of  $R = 0.3$  about the photon is less than 4 GeV. Moreover, we assume that a photon within the acceptance is detected with an efficiency of 80% (100%) if its energy is smaller (greater) than 25 GeV. In our analysis, we neglect multiple scattering effects as well as any detector-dependent effects such as lepton, photon or jet misidentification. Finally, in our simulation, we have not incorporated the finite decay length of the  $\tilde{\chi}_1^0$  but assumed that the  $\tilde{\chi}_1^0$  decays at the production vertex. This will introduce some small error in the direction of the photons from the decays  $\tilde{\chi}_1^0 \rightarrow \gamma$  for our choice of  $M = 500$  TeV. Although the displacement of the  $\tilde{\chi}_1^0$  decay vertices should be properly included in a complete simulation, we see from Fig. 6 that over most of the parameter range for which we have performed our simulation, the decay length is a fraction of a centimetre so that the results we show below should not be qualitatively altered.

## B . Classification of Events and Topological Cross Sections

We classify G M L E S B signals at the Tevatron primarily by the number of isolated photons, and then further separate them by their lepton content. We also distinguish events which do or do not contain jets.

In addition to a global cut  $E_T > 30$  GeV, we require that every event must satisfy at least one of the following lepton, photon or jet requirements which are motivated by the need for a trigger:

1` with  $p_T(\ell) > 20$  GeV, or 2` with  $p_T(\ell) > 10$  GeV;

two isolated photons;

two jets with  $E_T > 30$  GeV and  $E_T > 40$  GeV.

The results of our calculations of the cross sections for various event topologies after imposing the cuts and "trigger requirements" described above are shown in Fig. 8-Fig. 11

as a function of the parameter  $\tan\beta$ . We have once again fixed  $M = 500$  TeV and shown these cross sections for  $\tan\beta = 2$  and 10, and both signs of  $\mu$  as in Fig. 5. For each choice of  $\tan\beta$  and  $\mu$  we show the cross sections for events with (a) no identified photons, (b) 1  $\gamma$ , and (c) 2  $\gamma$ . The solid lines show the cross section for events with jets, while the dotted lines show the cross sections for "clean" events free of jet activity. We have performed event simulations for values of  $\sqrt{s}$  between 40–140 TeV in steps of 20 TeV and denoted the cross sections for  $n$ -lepton events by the symbol  $\sigma_n$  in the figures. The following remarks about Fig. 8–Fig. 11 are worth noting:

1. For all the four combinations of  $\tan\beta$  and  $\text{sgn}(\mu)$  shown in these figures, we see that cross sections for events with jets dominate the cross sections for clean events. This is because over most of the parameter space,  $\tilde{W}_1\tilde{Z}_2$  and  $\tilde{W}_1\tilde{W}_1$  are the dominant sparticle production mechanisms, and at least  $\tilde{W}_1$  typically has a large branching fraction for hadronic decays. For the smaller values of  $\sqrt{s}$  shown in the figure,  $\tilde{Z}_2 \rightarrow \nu_R \nu_R$  is the only two body decay channel that is kinematically allowed, so that the leptonic decays of  $\tilde{Z}_2$  dominate. As  $\sqrt{s}$  becomes larger, the decays  $\tilde{Z}_2 \rightarrow Z\tilde{Z}_1$  and  $\tilde{Z}_2 \rightarrow H_1\tilde{Z}_1$  become accessible and dominate the decay to right-handed sleptons, so that  $\tilde{Z}_2$  then mainly decays via its hadronic mode. This also accounts for why the dotted lines in Fig. 8–Fig. 11 exhibit a steeper fall-off than their solid counterparts.
2. Most of the dilepton plus multijet events contain opposite sign dileptons in this case because contributions to the signal from  $\tilde{g}\tilde{g}$  and  $\tilde{g}\tilde{q}$  production are subdominant (see Fig. 7) since gluinos and squarks tend to be heavy.
3. We see that for the jetty event sample, the cross section for 1  $\gamma$  events is larger by a factor 1.5–4 than the cross sections in the 0 or 2 photon event samples. This is, of course, sensitive to our assumptions about the  $\gamma$  acceptance ( $\eta_\gamma < 1$ ) and detection efficiency and could be different for Run II of the Tevatron.
4. For the case of the clean events shown in the figures, we see that cross sections where both photons are observed tend to be larger than those where the photons escape detection. This is presumably because it is easier for the photons to satisfy the isolation requirements than in the case of jetty events.
5. A comparison of the four figures shows that the various cross sections vary rather weakly with  $\tan\beta$  but show slightly more sensitivity to  $\text{sgn}(\mu)$  (when  $\tan\beta$  is not large).

We have not made an attempt to compute SM backgrounds to the SUSY event sample from the GMSB model. Background levels for the zero photon sample in case (a) shown in these figures have been previously estimated [27], although not with precisely the same cuts. We surmise that the presence of additional isolated photons, and possibly, also the presence of up to two significantly displaced vertices (without charged tracks emerging from them) would reduce the physics backgrounds to negligible levels. Of course, a careful computation that includes the effects of the non-zero decay length of the NLSP should ultimately be carried out to ensure there are no unforeseen surprises.

Assuming that the signal is indeed rate-limited, we estimate the SUSY reach of the Tevatron for an integrated luminosity of (i)  $100 \text{ pb}^{-1}$ , corresponding to the size of the

Run I data sample per experiment, (ii)  $2 \text{ fb}^{-1}$ , the integrated luminosity expected to be accumulated after about two years of Main Injector operation at design luminosity, and finally, (iii)  $25 \text{ fb}^{-1}$ , the integrated luminosity that might optimistically be accumulated at the proposed TeV 33 upgrade [18] of the Tevatron. For our estimate of the Run I and Run II reach, we take the 5 signal event level as our criterion for observability in any one channel, while for TeV 33, we take the observability level to be 10 events, and show the corresponding cross sections by the horizontal dashed lines in the figure. We see that when the data from Run I is analysed, the CDF and D0 experiments will be probing  $\sqrt{s}$  values of 50–60 TeV. With the Main Injector, experiments at the Tevatron should be able to explore up to  $\sqrt{s} \approx 100 \text{ TeV}$ . If TeV 33 is able to accumulate a data sample of  $25 \text{ fb}^{-1}$ , then the reach should extend out to about 135 TeV. For comparison with earlier studies of the Tevatron reach, these reach numbers correspond to  $m_{\tilde{g}}$  values of 450; 800 and 1100 GeV. In contrast to the mSUGRA case [27, 18, 28, 29], we find here that the reach via the clean channels is smaller than via jetty channels. It should, of course, be remembered that we are not directly probing such massive gluinos at the Tevatron, but obtaining the signal via the chargino and neutralino channels. Also, we remind the reader that our estimate of the reach may be somewhat optimistic since we have assumed that backgrounds are completely negligible: there could be important detector-dependent backgrounds that may not be ignorable. On the other hand, the reach could be even larger than our estimate if we sum up the expected signal in the many different channels.

Before closing this discussion, we remark upon the various attempts in the literature [12, 14] to account for the  $e^+e^-$  event by the CDF collaboration [15] within the GMLESB framework. We see from Fig. 8–Fig. 11 that while it is indeed possible to have a cross section of about 10 fb for clean dilepton plus two photon events (corresponding to  $\approx 1$  event in the Run I data), this event should have been accompanied by at least an order of magnitude (and possibly, as many as fifty) times as many events in other channels. For this reason, we feel that this interpretation of the CDF event is unlikely at least within this minimal framework.

We should mention, however, that it is possible to reduce the ratio of slepton to electroweak gaugino masses by increasing the number of  $5 + \bar{5}$  fields in the messenger sector. This cannot be larger than four if gauge couplings are to remain perturbative up to the GUT scale, but it is possible to arrange for  $\tilde{W}_1 \rightarrow \tilde{\chi}_L^\pm \gamma$  and  $\tilde{Z}_2 \rightarrow \tilde{\chi}_1^0 \gamma$  to be the only two body decays of the charginos and neutralinos if  $\beta$  is not large. In this case, the hadronic signals from  $\tilde{W}_1$  and  $\tilde{Z}_2$  production would be greatly reduced [30]. It would be of interest to simulate such a scenario to see whether it is possible for the dominant signal to be in the  $\tilde{\chi}_1^\pm \tilde{\chi}_1^0$  channel. But we stress that it is necessary to check all other signals that are likely to be present before attributing the CDF event to sparticle production within the GMLESB picture.

#### IV. SUMMARY AND CONCLUDING REMARKS

During the last year or two, we have witnessed the emergence of a phenomenologically viable alternative to the minimal SUGRA model for analyses of supersymmetry. This new scenario is similar to SUGRA in that SUSY is dynamically broken in a hidden sector of the theory which does not couple to the known particles and their superpartners via SM gauge interactions. Effects of SUSY breaking are communicated to the known particles via SM

gauge interactions with a messenger sector which also couples to the hidden sector. The difference is that while gravity plays the role of the messenger within the SUGRA framework, new sets of messenger fields are invoked in these novel scenarios. Thus, while the messenger scale is necessarily  $O(M_{\text{Planck}})$  for SUGRA models, this scale may be as small as a few hundred TeV within the novel GMLESB scenario.

From a phenomenological point of view, the SUGRA and GMLESB scenarios differ in two crucial respects. First, the boundary conditions for the RGE that determine the weak scale parameters of the theory are different: in the mSUGRA case, we have universal parameters at a scale  $M_{\text{GUT}}$ , while in the GMLESB case, sparticle masses, which are radiatively generated at the messenger scale are proportional to the SM gauge couplings squared. As a result, sparticles with the same gauge quantum numbers have the same masses (unless they have large Yukawa type interactions) so that flavour changing neutral currents are automatically suppressed. Second, unlike the mSUGRA framework where the lightest neutralino is the LSP and the gravitino decouples from particle physics, the gravitino is superlight within the GMLESB scenario and  $\tilde{\chi}_1$  decays into a gravitino and a photon (or, possibly also a Higgs or Z boson). For sparticles in the mass range accessible at the Tevatron, only the photon decays of  $\tilde{\chi}_1$  are significant, so that every SUSY event contains two isolated hard photons (though these may not both be detected).

In Section II we have set up the parameter space for the simplest GMLESB scenario and examined the extent that this has directly been probed by experiments at high energy colliders or indirectly via the effects of virtual sparticles on the flavour changing decay  $b \rightarrow s$ . We have also shown that a measurement of the decay length of the  $\tilde{\chi}_1$  yields information about the messenger scale.

The main purpose of this paper was to study the cross sections for various event topologies that should be accessible at the Tevatron within the minimal GMLESB picture. Towards this end we have interfaced the weak scale SUSY parameters obtained from these boundary conditions with ISAJET to obtain these cross sections. We believe that our calculations are the first semi-realistic simulations performed within this framework. Our main results are exhibited in Fig. 8-Fig. 11 for experimental conditions suitable at the Tevatron. We see that, unlike in SUGRA where multijet plus  $E_T$  events form the dominant event topology, multijet plus  $n = 0; 1; 2$  plus 1 photon events are the major component of the SUSY cross section. Similar events with two isolated photons or zero photons, which have only a slightly smaller cross section, may also be present at observable levels even in the Run I data sample (and certainly at the Main Injector upgrade) if any observation in the single photon channel is to be attributed to the minimal GMLESB realization of SUSY. It should be kept in mind that the relative sizes for the  $0:1:2$  cross sections are sensitive to our assumptions about the photon acceptance and detection efficiency. We also see that the cross section for clean multileptons plus photon event topologies is below our level of detectability during the current run: a handful of such events may, however, be present in the CDF and D0 Run I data samples if  $\sqrt{s}$  is not too large. At the Main Injector, up to several tens of clean and  $\tilde{\chi}_1$  plus multiple lepton events may be present. While the reach extends out to about

50–60 TeV for Run I experiments, the Main Injector (TeV 33) should be able to probe up to 100 TeV (135 TeV), which corresponds to  $m_g \approx 800$  GeV (1 TeV)!

How stable are our conclusions to model variations? We note that there is a small region of parameter space (the cross-hatched region in Fig. 2) where  $\tilde{\chi}_1$  is the NLSP. For parameters

in this region, all SUSY events will contain at least 2-4 leptons but no photons in the final state. We note that the phenomenology may be sensitive to assumptions about the messenger sector. For instance, if instead of assuming that it contains a single vector multiplet of SU(5), if instead we assume it contains four such multiplets (coupling roughly the same way), then slepton and squark masses reduce by about half relative to the electroweak gaugino and gluino masses. This could have a significant impact on sparticle decay patterns and the resulting phenomenology.

In summary, we have examined the implications for experiments at the Tevatron in a new class of models where SUSY is broken at relatively low energy, and the effects of SUSY breaking communicated by gauge interactions. The production of sparticles at the Tevatron would then result in a variety of events with  $n$ -jets +  $m$ -leptons +  $k$ -photons +  $E_T$ . We have computed the cross sections for these event topologies under experimental conditions appropriate to the Tevatron, and mapped out its reach within the parameter space of the model for both the current run as well as the Main Injector (and TeV33) upgrades. Observation of these events would not only be spectacular in that it would signal the discovery of a fundamental new symmetry of Nature, but also in that it would imply the existence of a whole new family of particles not very far beyond the multi-TeV scale. In contrast to the case of the desert hypothesis, we would have a hope of directly probing this sector in the foreseeable future. In the meantime, we might be able to obtain [31] indirect information about the physics of this sector via the experimental determination of masses and other properties of sparticles.

#### ACKNOWLEDGMENTS

We are grateful to our colleagues in the Theory Subgroup of the Supersymmetry Working Group at Snowmass96, especially Scott Thomas and J. Lykken for valuable discussions and sharing their insights. We also thank T. ter Veldhuis for discussions and comments. C. H. Chen thanks the HEP group at Florida State University for hospitality while this work was completed. This research was supported in part by the U.S. Department of Energy under contract number DE-FG 05-87ER 40319, DE-FG 03-91ER 40674 and DE-FG -03-94ER 40833.

NOTE ADDED: While this paper was in preparation, we received two papers [32,33] where the spectroscopy and the phenomenology of the minimal GMLESB model as well as of models with extended messenger sectors is considered. While parts of these papers overlap with the present work, neither of these papers performed explicit event generation for the GMLESB model for the Tevatron collider.

## REFERENCES

- [1] H. P. Nilles, *Phys. Rep.* 110, 1 (1984); H. Haber and G. Kane, *Phys. Rep.* 117, 75 (1985); X. Tata, in *The Standard Model and Beyond*, p. 304, edited by J. E. Kim, *World Scientific* (1991); R. Arnowitt and P. Nath, *Lectures presented at the VII J. A. Swieca Summer School, Campos do Jordao, Brazil, 1993 CTP-TAMU-52/93*; V. Barger and R. J. N. Phillips, in *Recent Advances in the Superworld*, J. Lopez and D. Nanopoulos, Editors, *World Scientific* (1994); *Properties of SUSY Particles*, L. Cifarelli and V. Khoze, Editors, *World Scientific* (1993); J. Bagger, *Lectures presented at TASI95, University of Colorado at Boulder, Johns Hopkins preprint, JHU-TIPAC-96008, hep-ph/9604232* (1996); X. Tata, *Lectures presented at TASI95, University of Colorado at Boulder, Hawaii preprint UH-511-833-95 hep-ph/9510287* (1995).
- [2] A phenomenological summary of the current experimental situation as well as a survey of the reach of various colliders may be found in H. Baer et. al., to appear in *Electroweak Symmetry Breaking and New Physics at the TeV Scale*, edited by T. Barklow, S. Dawson, H. Haber and J. Seigrist, (*World Scientific*) 1995.
- [3] For a recent review, see M. Drees and S. Martin, to appear in *Electroweak Symmetry Breaking and New Physics at the TeV Scale*, edited by T. Barklow, S. Dawson, H. Haber and J. Seigrist, (*World Scientific*) (1995); for a rapid survey of other models, see J. Amundson et. al. *hep-ph/9609374* (1996).
- [4] D. Buskulic et. al., *CERN preprint, CERN-PPE/96-083* (1996); A. Lyon, talk presented at the 1996 Division of Particles and Fields Meeting, Minneapolis, MI (August, 1996).
- [5] R. Arnowitt, A. Chamseddine and P. Nath, *Phys. Rev. Lett.* 49, 970 (1982) and *Phys. Rev. Lett.* 50, 232 (1983); R. Barbieri, S. Ferrara and C. Savoy, *Phys. Lett. B* 119, 343 (1982); L. Hall, J. Lykken and S. Weinberg, *Phys. Rev. D* 27, 2359 (1983).
- [6] S. Deser and B. Zumino, *Phys. Rev. Lett.* 38, 1433 (1977); E. Cremmer et. al. *Phys. Lett. B* 79, 231 (1978).
- [7] See, e.g. J. Bagger, Ref. [1]
- [8] L. Ibanez and G. Ross, *Phys. Lett. B* 110, 215 (1982); L. Ibanez, *Phys. Lett. B* 118, 73 (1982); K. Inoue et. al. *Prog. Theor. Phys.* 68, 927 (1982) and 71, 413 (1984). J. Ellis, D. Nanopoulos and K. Tamvakis, *Phys. Lett. B* 121, 123 (1983); L. Alvarez-Gaume, J. Polchinski and M. Wise, *Nucl. Phys. B* 221, 495 (1983).
- [9] Some recent papers include M. Drees and M. Nojiri, *Phys. Rev. D* 47, 376 (1993) and H. Baer and M. Bhlik, *Phys. Rev. D* 53, 597 (1996); for a recent review, see G. Jungman, M. Kamionkowski and K. Griest, *Phys. Rep.* 267, 195 (1996).
- [10] M. Dine and A. Nelson, *Phys. Rev. D* 48, 1277 (1993); M. Dine, A. Nelson, Y. Shirman, *Phys. Rev. D* 51, 1362 (1995); M. Dine, A. Nelson, Y. Nir and Y. Shirman, *Phys. Rev. D* 53, 2658 (1996).
- [11] P. Fayet, *Phys. Lett. B* 70, 461 (1977).
- [12] S. Dimopoulos, M. Dine, S. Raby and S. Thomas, *Phys. Rev. Lett.* 76, 3494 (1996); S. Dimopoulos, S. Thomas and J. Wells, *Phys. Rev. D* 54, 3283 (1996).
- [13] S. Ambrosanio et. al., *Phys. Rev. Lett.* 76, 3498 (1996) and *hep-ph/9605398* (1996).
- [14] K. S. Babu, C. Kolda and F. Wilczek, *Princeton preprint, IASSNS-HEP 96/55, hep-ph/9605408* (1996).
- [15] S. Park, *Search for New Phenomena in CDF in 10th Topical Workshop on Proton-*

- Antiproton Collider Physics, R. Raha and G. Yodh, Editors (AIP Press, New York 1995).
- [16] G. Dvali, G. Giudice and A. Pomarol, CERN preprint, CERN-TH/96-61, hep-ph/9603238 (1996).
  - [17] F. Paige and S. Protopopescu, in Supercollider Physics, p. 41, ed. D. Soper (World Scientific, 1986); H. Baer, F. Paige, S. Protopopescu and X. Tata, in Proceedings of the Workshop on Physics at Current Accelerators and Supercolliders, ed. J. Hewett, A. White and D. Zeppenfeld, (Argonne National Laboratory, 1993), hep-ph/9305342.
  - [18] Future Electroweak Physics at the Tevatron, D. Amidei and C. Brock, Editors, FERMILAB-Pub-96/082 (1996).
  - [19] If the messenger sector was strongly coupled, the gauginos would have obtained a large mass while the scalars would have obtained masses given by  $m_{\text{scalar}}^2 \propto m_{\text{mess}}^2$ , and the resulting phenomenology would have been quite different [12].
  - [20] Radiative generation of gaugino masses was considered in, see M. Dine, W. Fischler and M. Srednicki, Nucl. Phys. B 189, 575 (1981); S. Dimopoulos and S. Raby, Nucl. Phys. B 192, 353 (1982); M. Dine and W. Fischler, Nucl. Phys. B 204, 346 (1982); L. Alvarez-Gaume, M. Claudson and M. Wise, Nucl. Phys. B 207, 96 (1982).
  - [21] Talk by J. Nachtman (ALEPH Collaboration) at DPF96 meeting.
  - [22] M. S. Alam et. al., Phys. Rev. Lett. 74, 2885 (1995).
  - [23] H. Baer and M. Brhlik, FSU-HEP-961001 (1996), hep-ph/9610224.
  - [24] The AMY Collaboration (Y. Sugimoto et. al, Phys. Lett. B 369, 86 (1996)), in their search for single photon events at TRISTAN requires that the photon points to the interaction region. The resolution, which presumably improves with increasing photon energy, quoted in this analysis is 4.4 cm : for 6 GeV photons, and is derived from the angular resolution of about  $2.5^\circ$ . Assuming that SUSY events can be triggered via jets or leptons, the calorimeter segmentation would allow for the determination of the photon impact parameter in the D0 experiment with a resolution of a few centimetres if  $\tilde{\chi}_1$  decays before, or within, the electromagnetic calorimeter; this resolution would be somewhat degraded for decays within the hadronic calorimeter. A measurement of photon energy would not be possible if  $\tilde{\chi}_1$  decayed in the muon chamber. We thank Mike Jones, Mike Peters and Steve Olsen for discussions about this issue.
  - [25] J. Botts et. al., Phys. Lett. B 304, 159 (1993).
  - [26] We have checked, for example that for  $M = 500$  TeV the width for  $\tilde{\chi}_2$  decays into a gravitino varies between  $5 \cdot 10^4 - 10^2$  eV for the four cases (a)-(d) and for the entire range of  $\mu$  that we have considered in Fig. 2. This is to be compared to the decay width into other SUSY modes which is typically  $O(M \text{ eV})$  ( $O(\text{keV})$ ) for two-body (three-body) decays of  $\tilde{\chi}_2$ .
  - [27] See e.g. H. Baer, C-H. Chen, F. Paige and X. Tata, FSU-HEP-960415, hep-ph/9604406 (1996), Phys. Rev. D (in press),
  - [28] S. Mrenna, G. Kane, G. D. Kribs and J. D. Wells, Phys. Rev. D 53, 1168 (1996).
  - [29] T. Kamon, J. Lopez, P. McIntyre and J. T. White, Phys. Rev. D 50, 5676 (1994).
  - [30] We have explicitly computed the sparticle production cross sections with RGE boundary conditions for the extreme case where there are four  $5 + 5$  messenger multiplets. Since (for the same choice of  $\mu$ ) sparticles are heavier than in the minimal case studied in the text, values as small as 10 TeV are now consistent with the data. For  $\mu = 20$  TeV

which yields a production cross section  $\sim 100$  fb before any cuts, we find that the production of sleptons is comparable to, or at most 2-3 times higher, than  $\tilde{W}_1$  and  $\tilde{Z}_2$  production. We have explicitly checked that for these scenarios, leptonic decays of charginos and neutralinos dominate, so that SUSY signals would indeed be dominated by events without any jet activity.

- [31] M. Peskin, to appear in Proc. of Yukawa International Seminar, Kyoto, Japan, August 1995, hep-ph/9604339 (1996).
- [32] S. Dimopoulos, S. Thomas and J. Wells, SLAC preprint, SLAC-PUB-7237, hep-ph/9609434 (1996).
- [33] J. Bagger, K. Matchev, D. Pierce and R. Zhang, Johns Hopkins preprint, JHU-TIPAC-96018, hep-ph/9609444 (1996).



## FIGURES

FIG .1. Renormalization group trajectories for the soft SUSY breaking scalar masses and the gaugino masses  $M_i$  versus renormalization scale  $Q$  from the messenger scale ( $M = 500$  TeV) to the weak scale. In this example, we take  $m_0 = 40$  TeV,  $\tan\beta = 2$ ,  $\mu < 0$  and  $m_t = 175$  GeV.

FIG .2. Contours of  $\tilde{\gamma}_R$  (solid),  $\tilde{\gamma}_L$  (dashed) and  $\tilde{Z}_1$  (short-dashed) and  $\tilde{W}_1$  (dotted) masses in the  $\mu$  vs:  $\tan\beta$  plane of the GMLESB model with a single  $5+5$  representation in the messenger sector for a)  $\mu < 0$  and b)  $\mu > 0$ . We also show contours for  $m_{\tilde{g}}$  (solid),  $m_{\tilde{q}}$  (dashed),  $A_t$  (short-dashed) and  $A_b$  (dotted) for c)  $\mu < 0$ , and d)  $\mu > 0$ . We take  $m_t = 175$  GeV and  $M = 500$  TeV. The bricked regions are excluded by theoretical constraints discussed in the text, while the shaded regions are excluded by experiment. The cross-hatched region is where  $\tilde{\gamma}_1$  is the NLSP.

FIG .3. Contours of the branching fraction ( $\times 10^4$ ) for the decay  $b \rightarrow s \tilde{\gamma}$  in the  $\mu$  vs:  $\tan\beta$  plane for  $M = 500$  TeV, for a)  $\mu < 0$ , and b)  $\mu > 0$ . The CLEO experiment has measured this branching fraction to be between  $(1.4 \pm 2) \times 10^{-4}$  at 95% CL.

FIG .4. Contours of the value of the  $B$  parameter as obtained from the conditions of electroweak symmetry breaking but evolved to the messenger scale taken to be 500 TeV for a)  $\mu < 0$  and b)  $\mu > 0$ . If there are no new interactions, the value of this parameter should be small so that the model taken literally picks out  $\mu < 0$  and  $\tan\beta = 20-30$ . See the text for a further discussion of this point.

FIG .5. Branching fractions of the lightest neutralino  $\tilde{Z}_1$  decays to the gravitino versus  $\mu$  for a)  $\tan\beta = 2$ ;  $\mu < 0$ , b)  $\tan\beta = 2$ ;  $\mu > 0$ , c)  $\tan\beta = 10$ ;  $\mu < 0$  and d)  $\tan\beta = 10$ ;  $\mu > 0$ . The messenger scale is fixed to be 500 TeV.

FIG .6. The decay length in centimeters of the lightest neutralino  $\tilde{Z}_1$  decays to the gravitino versus  $\mu$  for a)  $\tan\beta = 2$ ;  $\mu < 0$ ,  $M = 500$  TeV and b)  $\tan\beta = 2$ ;  $\mu < 0$ ,  $M = 5000$  TeV. The three curves from bottom to top for  $\tilde{g}_{11} = 1.5$ ; 2 and 4. Frames c) and d) are identical to a) and b) above except that  $\mu > 0$ .

FIG .7. Total production cross sections for sparticles in the GMLESB scenario for the Tevatron collider operating at  $\sqrt{s} = 2$  TeV. We show frames for a)  $\tan\beta = 2$ ;  $\mu < 0$ , b)  $\tan\beta = 2$ ;  $\mu > 0$ , c)  $\tan\beta = 10$ ;  $\mu < 0$  and d)  $\tan\beta = 10$ ;  $\mu > 0$ . "Oth." refers to other chargino and neutralino processes and "Ass." refers to the production of a chargino/neutralino in association with a gluino/squark.

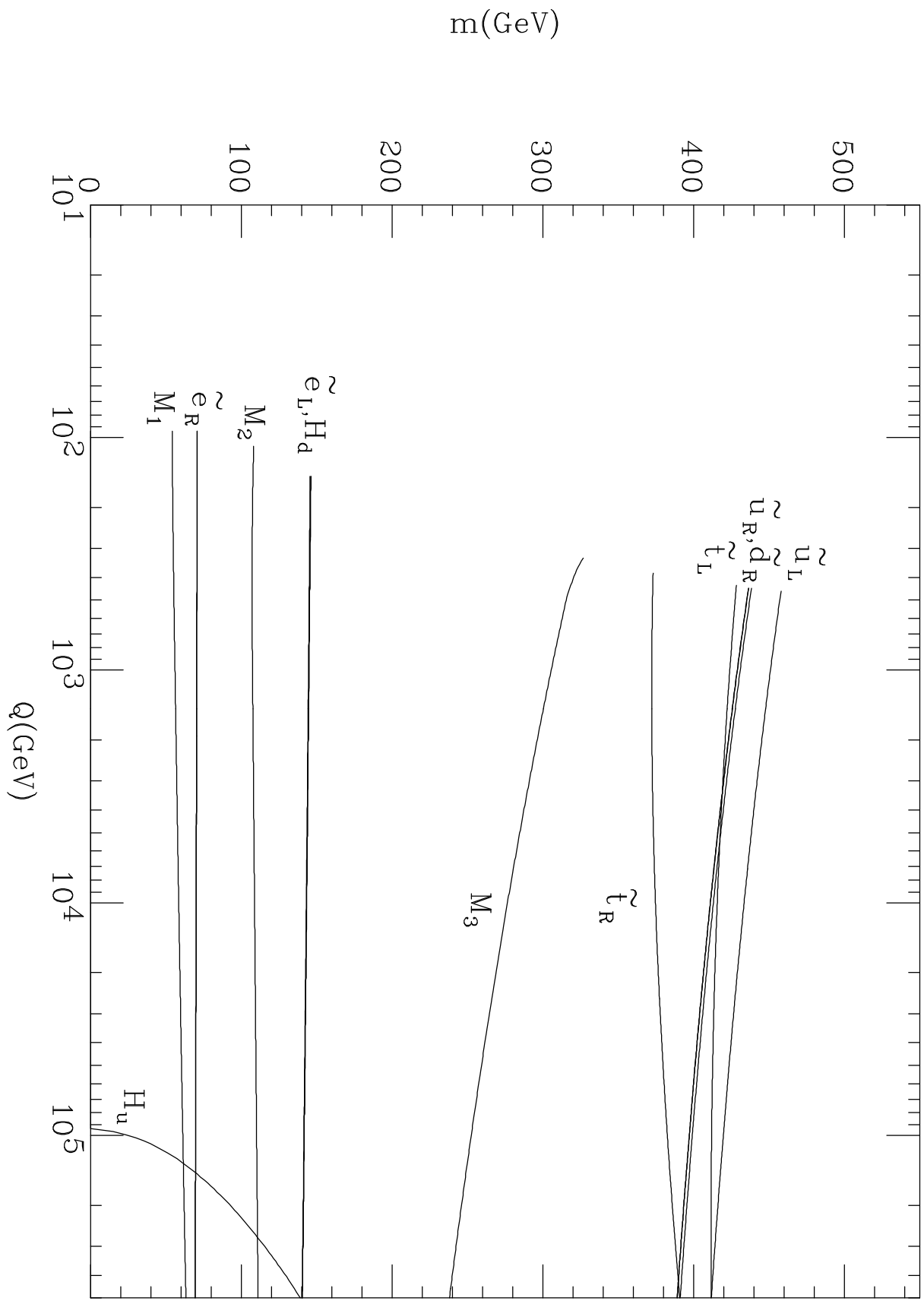
FIG .8. Topological cross sections from sparticle production and decay versus  $\tan\beta$  in the GM LESB framework for the Tevatron collider operating at  $\sqrt{s} = 2$  TeV with cuts and trigger conditions listed in the text. The messenger scale is fixed to be 500 TeV. We take  $\tan\beta = 2$  and  $\mu < 0$ . We show frames for a) events containing no isolated photons, b) events containing a single isolated photon, and c) events containing two isolated photons. The solid curves correspond to events containing jets, while the dotted curves correspond to clean topologies (no jets). The curves are labelled according to the number of isolated leptons present in the signal. The dashed horizontal lines correspond to the approximate reach of the Fermilab Tevatron with 0.1, 2 and 25 fb<sup>-1</sup> of integrated luminosity with observability criteria listed in the text.

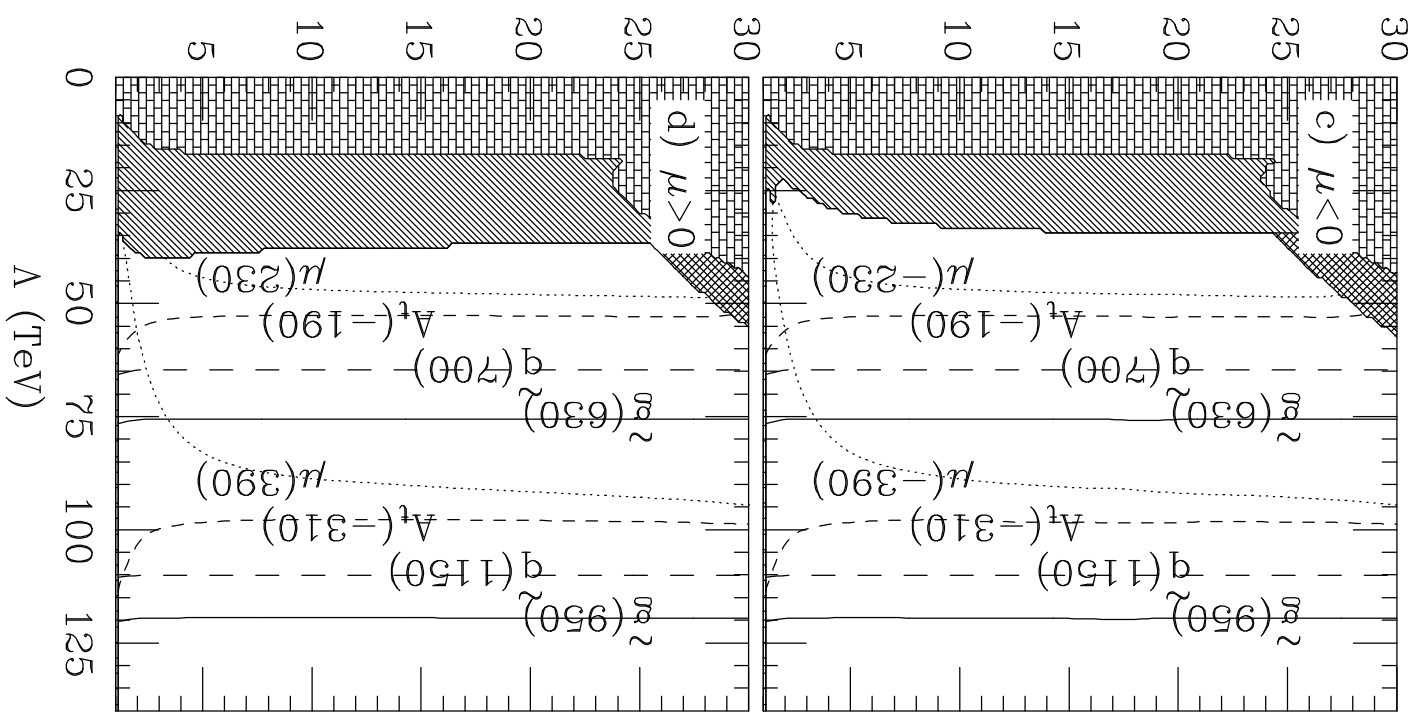
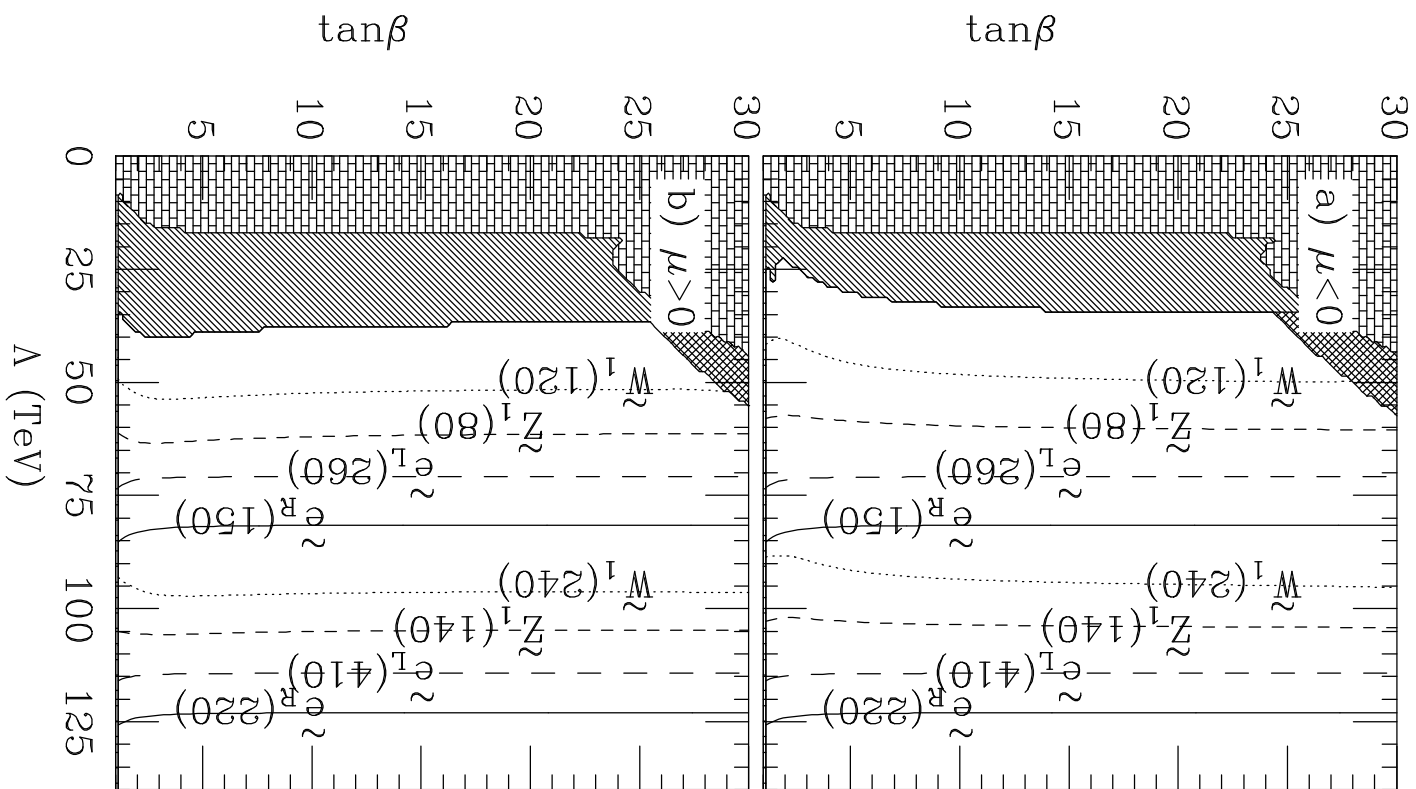
FIG .9. The same as Fig. 8 except that  $\tan\beta = 2$ ,  $\mu > 0$ .

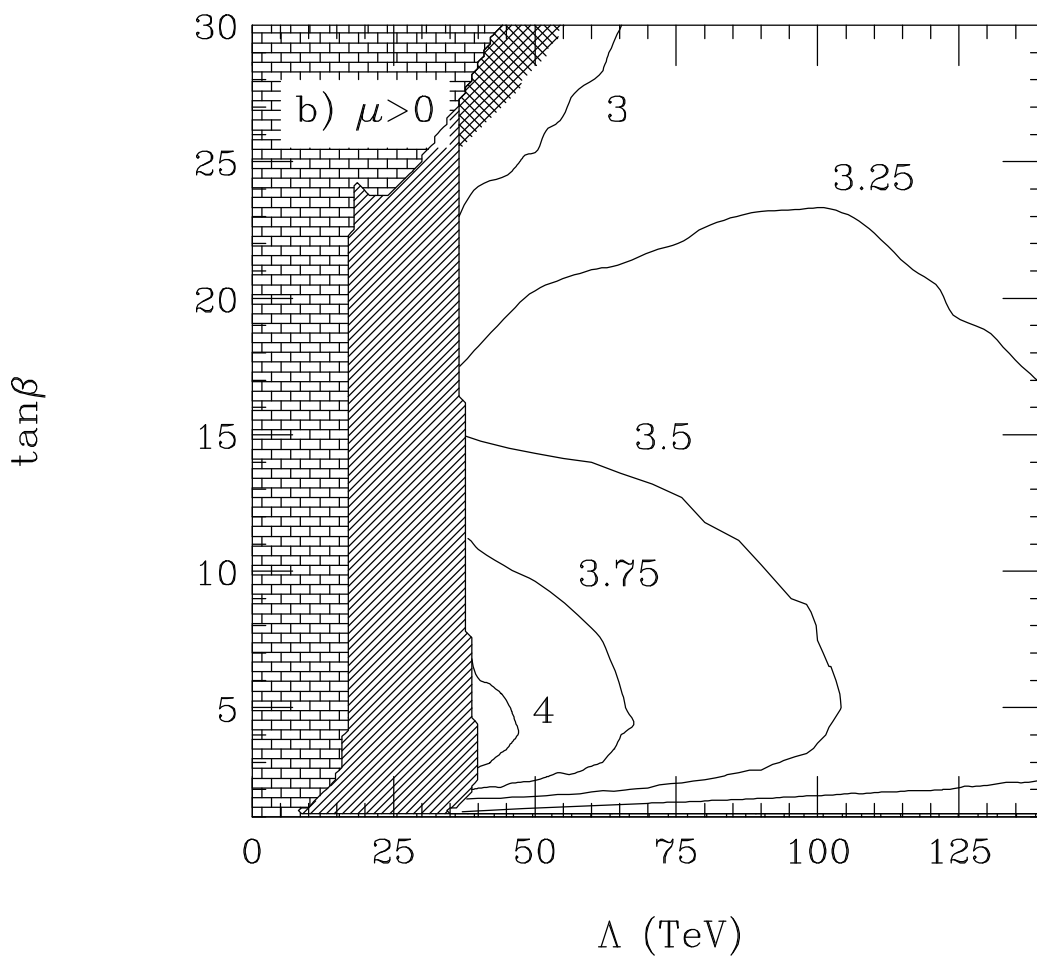
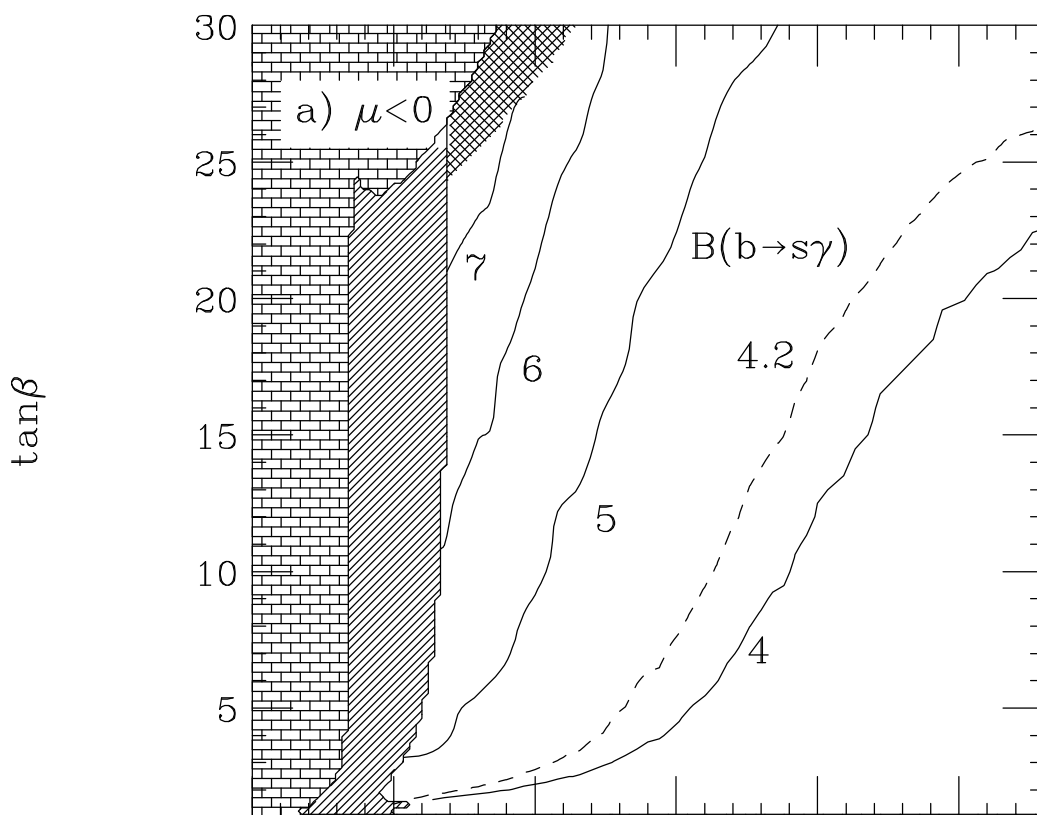
FIG .10. The same as Fig. 8 except that  $\tan\beta = 10$ ,  $\mu < 0$ .

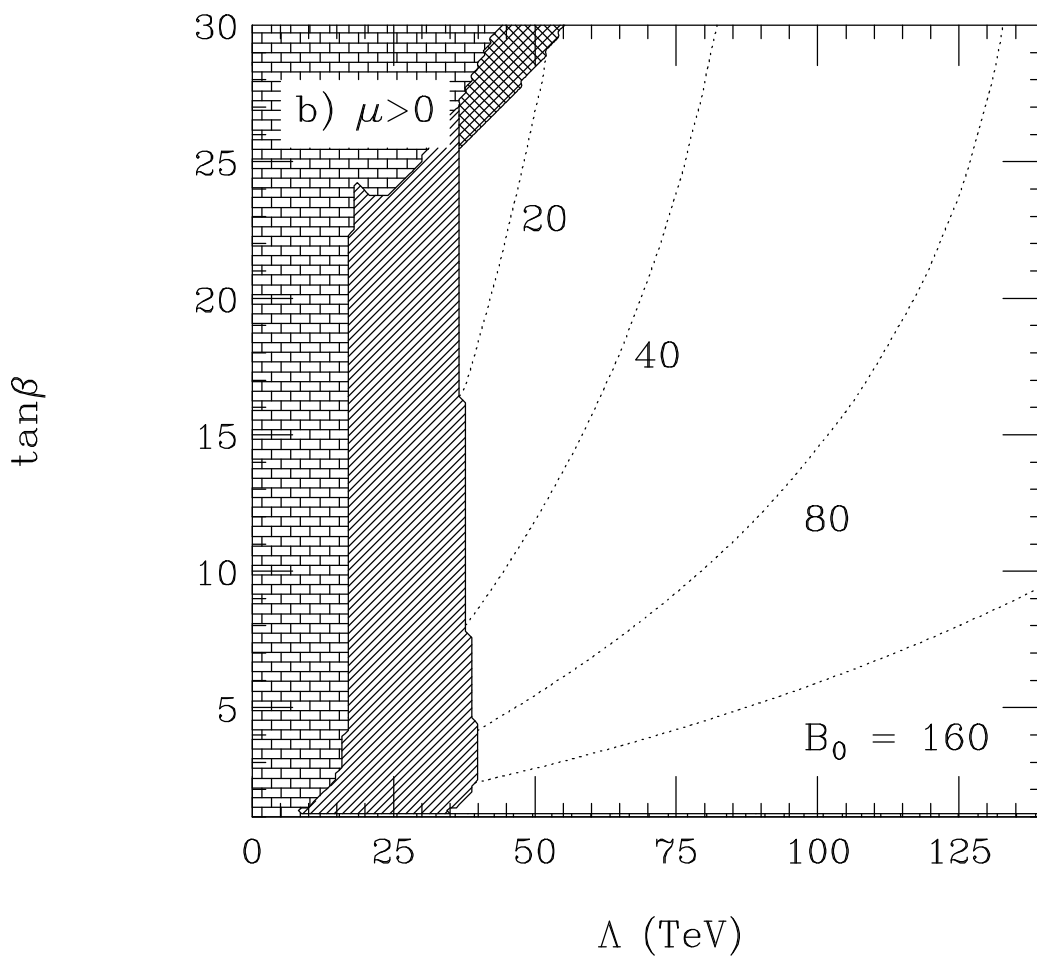
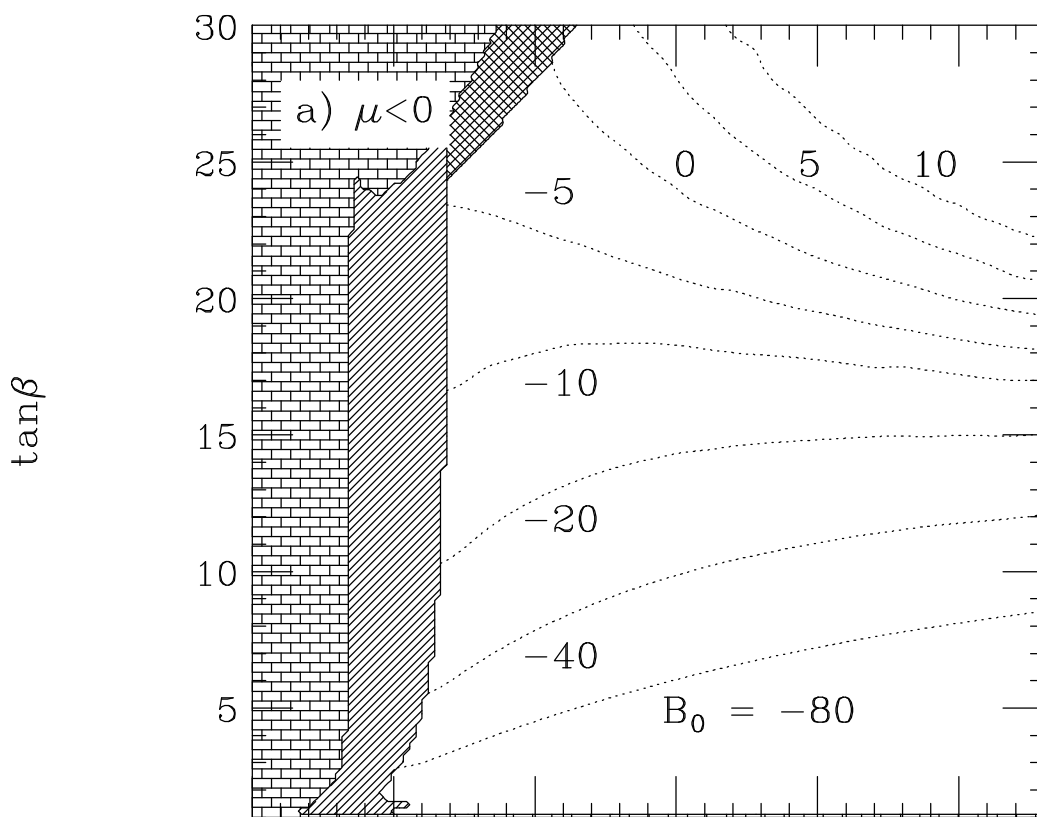
FIG .11. The same as Fig. 8 except that  $\tan\beta = 10$ ,  $\mu > 0$ .

$M=500$  TeV,  $\Lambda=40$  TeV,  $\tan\beta=2$ ,  $\mu<0$ ,  $m_t=175$  GeV

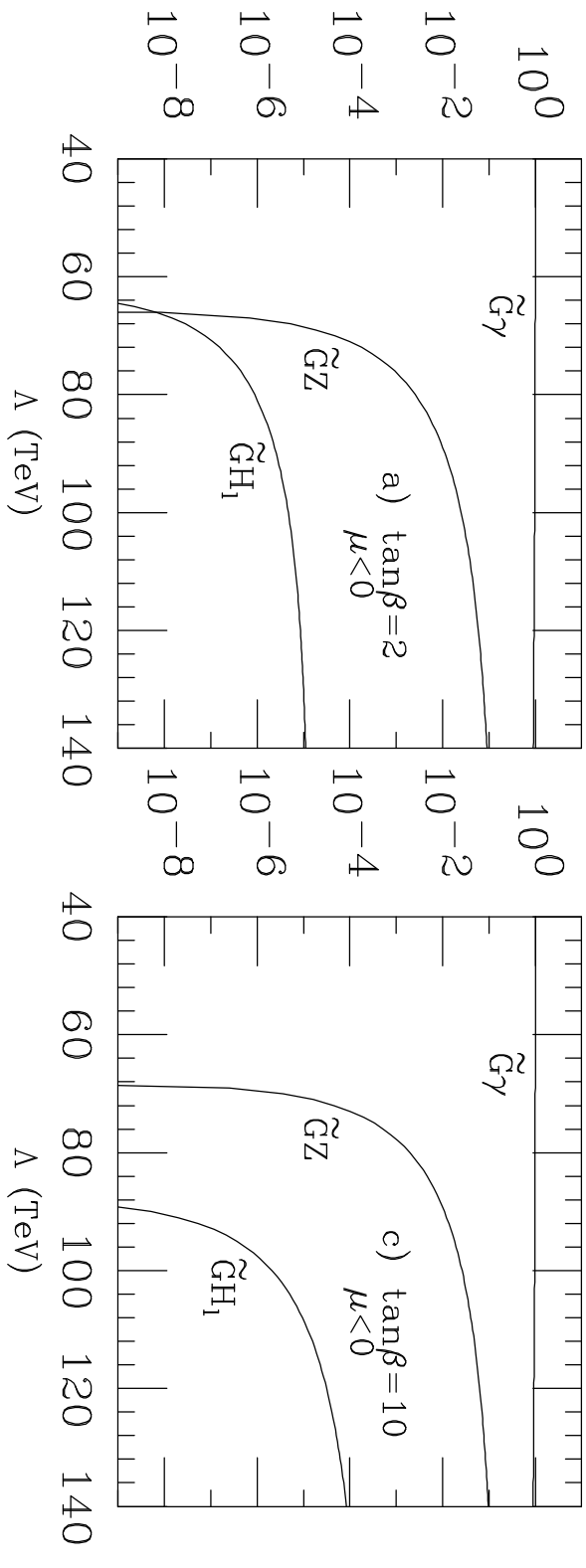








branching ratio of  $\tilde{Z}_1$



branching ratio of  $\tilde{Z}_1$

